A Topology-Optimized Large-Range Compliant X-Y Micro Stage

M.Dinesh[*] and G.K.Ananthasuresh
Mechanical engineering, IISc, Bangalore, India

[*] Corresponding author (email: mdinesh@mecheng.iisc.ernet.in)

Abstract

In this paper, we present a systematically obtained novel design of a compliant X-Y micro-stage with a large range of motion. Topology optimization is used to design a compliant mechanism for desired workspace by maximizing the displacement amplification along the X and Y axes. Geometrically nonlinear finite element analysis is used to model the behavior of the compliant mechanism using a ground structure of frame elements. The optimum design is found to cover a range of 6.57 % of the entire manipulator size. The stage is fabricated using wire-cut electro discharge machining (EDM) of spring steel (ENJ42/AISI1080) and it is actuated using shape memory alloy (SMA) wires.

Keywords: Micro Stage, Compliant mechanisms, Large Range, Wire-cut EDM, and SMA

1 Introduction

Most of the commercially available X-Y stages of large size are equipped with two mutually perpendicular, independent, and rigid-body linear actuators running in guide-ways. However, the presence of backlash, friction and wear in physical joints in these stages makes it inefficient and at times impossible to use the similar principles in micro and nano stages where high precision is desired. Compliant mechanisms (CMs), on the other hand, are backlash-free and joint-less. These and other advantages of compliant mechanisms over rigid body mechanisms make it appropriate to use CMs in high-precision instruments. Furthermore, the elastic nature of CM aids us in employing a very compact and often open-loop control for the stage.

Some efforts have been made in designing and analyzing CMs for high-resolution motions at the micro and nano sizes [1-3]. These efforts were focused on the design of CMs with flexural hinges. Flexural hinges are usually narrow (hourglass like) portions that imitate the kinematic revolute joints. The range of motion of such CMs is limited as the flexural hinges experience large stresses under large displacements. Some other designs of micro and nano positioning devices include the clever usage of thermo-mechanical actuators in order to achieve six degrees-of-freedom positioners [4], and positioning using impact forces [5]. Although high accuracy is achieved in positioning the above stages, many of them have limited range of operation either due to the usage of flexural hinges or due to the usage of actuators with low working range [6]. Some of them have serial arrangement in that one axis is stacked on top of another while others have parallel arrangement. It appears that all the aforementioned stages were conceived intuitively or were based on the experience of the designers. In this paper, we pose a structural topology optimization problem to get a parallel arrangement that has a large working range without purely relying upon intuition or experience. This enables us to design a stage by optimizing a quantifiable performance measures rather than based on only qualitative criteria. With respect to the literature on compliant mechanism synthesis, this paper treats a new problem of designing a CM for prescribed workspace.

Maximizing the workspace of a compliant mechanism implies that a chosen point (in this case, the motion stage) can move across a large area when two inputs are applied to the XY stage. An additional important requirement is to de-couple the motion of the stage due to the inputs applied in two orthogonal directions. Towards this, two objective functions suiting the above requirements are identified and a multi-objective optimization problem is posed (Section 2). Next, a common method of solving a multi-objective optimization problem is discussed briefly. Geometrically nonlinear analysis is briefly touched upon and a method of computing analytical sensitivities (which are required for the continuous optimization algorithm) is explained (Section 3). Finally, the results of the optimization procedure, a detailed discussion of the new compliant XY stage, and the actuation of the wire-EDM manufactured spring-steel prototype using SMA wires are discussed (Section 4 & 5).

2 Problem Statement

2.1 Specification

Consider a ground structure of frame elements with equal length in both X and Y directions as shown in Fig. (1-2). Three corner nodes, namely A, B and C are fixed to the ground and the forces are applied at points D and E as shown in the figures. The points D and E are allowed to move only in the X and Y directions respectively because the remaining degrees of freedom of these points are constrained by a folded beam suspension (FBS) attached at these points. This is done to enable independent movement of actuation point and is usually termed as actuator isolation [1]. The in-plane widths of all the members, except those of the FBS are the design variables for the op-

timization problem. All the beams are assumed to be made of spring steel (ENJ42/AISI1080) and the out-of-plane thickness of all members are same. A stage–elliptical disc– is connected to the remaining corner, F, of the square domain.

2.2 Optimization Problem

The workspace of the X-Y stage can be enhanced if the stage undergoes a large motion when forces are applied at D and E. However, the presence of FBS limits the motion of the input. Therefore, the range of the motion can be enhanced only by achieving displacement amplification from the input point to the CM and the output point. Furthermore, independent motions of the stage in both the X and Y directions for the forces applied at D and E is also desired. This simplifies the control system significantly. This is usually termed as stage isolation [1]. Therefore, the design problem can be posed as a multi-objective optimization given by

$$\underset{w}{Minimize} \left\{ \begin{array}{l} f_1 = f_{11} + f_{12} = -\left(\dfrac{u_{1,stage}}{u_{1,in}} + \dfrac{v_{2,stage}}{v_{2,in}} \right) \\[3mm] f_2 = f_{21} + f_{22} = \sqrt{\left(\dfrac{v_{1,stage}}{u_{1,in}} \right)^2} + \sqrt{\left(\dfrac{u_{2,stage}}{v_{2,in}} \right)^2} \end{array} \right\}$$

$$subject\ to \quad w_{lower} \le w_i \le w_{upper} \quad i = 1, 2, ..., n$$

where w is a vector containing the widths of all the frame members and n is the total number of frame members constituting the ground structure. Suffix "1" stands for the first load case where the mechanism is loaded along the X direction at the point D (see Fig. (1)) and "2" stands for the second load case in which case the force is only acting at the point E in the Y direction (see Fig. (2)). Here, we have $f_{11} = f_{12}$ and $f_{21} = f_{22}$ as a diagonal symmetry is considered for the design variable. Therefore, the problem can be modifies as

$$\underset{w}{Minimize} \left\{ \begin{array}{l} f_1 = f_{11} = -2\dfrac{u_{1,stage}}{u_{1,in}} = f_{12} = -2\dfrac{v_{2,stage}}{v_{2,in}} \\[3mm] f_2 = f_{21} = 2\sqrt{\left(\dfrac{v_{1,stage}}{u_{1,in}} \right)^2} = f_{22} = 2\sqrt{\left(\dfrac{u_{2,stage}}{v_{2,in}} \right)^2} \end{array} \right\}$$

$$subject\ to \quad w_{lower} \le w_i \le w_{upper} \quad i = 1, 2, ..., n \quad (1)$$

Objective function f_1 takes care of the amplification in both X and Y directions whereas the objective function f_2 takes care of decoupling the motion. All the n design variables are bounded between w_{lower} and w_{upper} to avoid the ill-conditioning of the stiffness matrix involved in the finite element analysis (FEA), which is required at every iteration of the optimization process. The quantities used in the expressions of functions f_1 and f_2 are defined in Figs. (1-2).

3 Solution Procedure

3.1 Multi-objective optimization

The most common, convenient, and simplest way of handling multi-objective optimization problems is the weighted sum method [7]. In the case of bi-objective problems, this assumes the form:

$$\underset{w}{Minimize} \quad F = \lambda f_1(w) + (1-\lambda) f_2(w) \quad 0 \le \lambda \le 1 \quad (2)$$

The weighting parameter λ is varied parametrically from 0 to 1 and the corresponding minimal points $\{f_1, f_2\}$ can be plotted to obtain the Pareto curve using which a desired Pareto minimal point can be chosen. Hence, we solve the optimization problem posed in Section 2.2 for several values of λ.
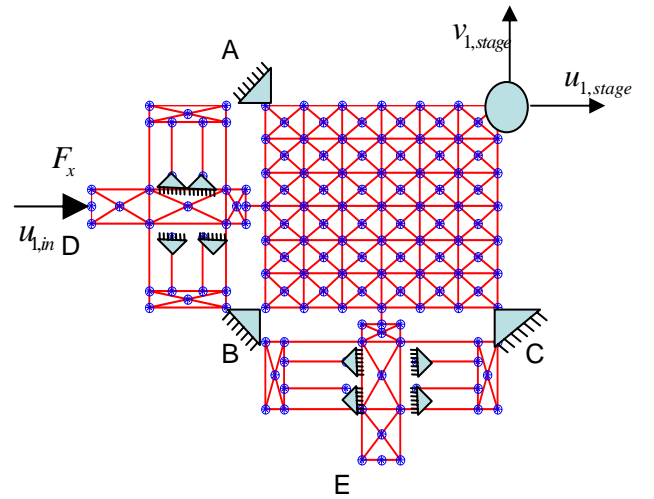

Figure 1: The ground structure of frame members. Force is applied at D in X direction to obtain a displacement of the stage in X direction.
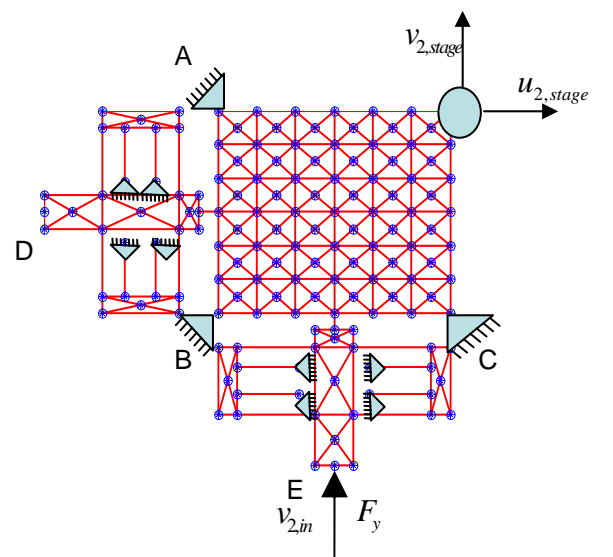

Figure 2: The ground structure of frame members. Force is applied at E in Y direction to obtain a displacement of the stage in Y direction.

3.2 Geometrically nonlinear FEA

Compliant mechanisms usually undergo large displacements and rotations but small strain [8]. This is commonly termed as geometrical nonlinearity where the FEA requires satisfying the equilibrium equation in the deformed configuration [9, 10]. In geometrically nonlinear FEA, the loads are applied in steps and a residual vector, g, is computed in each step.

$$g\left(x_0 + u\right) = f_{\text{internal}}\left(x_0 + u\right) - f_{\text{ext}} \qquad (3)$$

where $f_{\text{internal}}\left(x_0 + u\right)$ is the internal force vector, expressed in a global reference frame, depends on the initial configuration, x_0; and the net displacements u; and f_{ext} is the applied external force vector. $f_{\text{internal}}\left(x_0 + u\right)$ is computed using the equation:

$$f_{\text{internal}}\left(x_0 + u\right) + K_t\left(x_0 + u\right)\Delta u = f_{\text{ext}} + \Delta f_{\text{ext}} \qquad (4)$$

where Δu is the differential displacement vector; $K_t\left(x_0 + u\right)$ is tangent stiffness matrix; and these are computed using the equations

$$K_t\left(x_0 + u\right) = \frac{\partial g}{\partial u} = \frac{\partial f_{\text{internal}}}{\partial u} \qquad (5)$$

$$K_t\left(x_0 + u\right)\Delta u = \Delta f_{\text{ext}} \qquad (6)$$

3.3 Sensitivity Analysis

Most of the efficient optimization algorithms require the gradient of the objective function and the constraints with respect to the design variables to expedite the optimization process. In the case considered, since the objective function, F, is not an explicit function of the design variables, w, its derivative should be computed as

$$\frac{dF}{dw} = \frac{\partial F}{\partial u}\frac{du}{dw} \qquad (7)$$

In geometrically nonlinear case, the second term on the right hand side in Eq. (7) can be computed as

$$\frac{du}{dw} = -K_t^{-1}\sum_{i=1}^{n}\frac{\partial \Delta f_{\text{internal}}}{\partial w} \qquad (8)$$

where n is the total number of load steps. Therefore, we have:

$$\frac{dF}{dw} = \lambda\frac{df_1}{dw} + (1-\lambda)\frac{df_2}{dw} \qquad (9)$$

The first and second terms comprising the derivative can be computed from the following equations.

$$\frac{df_1}{dw} = \frac{df_{11}}{dw} \qquad (10)$$

$$\frac{df_2}{dw} = \frac{df_{21}}{dw} \qquad (11)$$

where

$$\frac{df_{11}}{dw} = \frac{-\left(u_{1,in}\dfrac{du_{1,stage}}{dw} - u_{1,stage}\dfrac{du_{1,in}}{dw}\right)}{u_{1,in}^{2}} \qquad (12)$$

$$\frac{df_{21}}{dw} = \frac{1}{f_{21}}\frac{\left(u_{1,in}^{2}\,v_{1,stage}\dfrac{dv_{1,stage}}{dw} - v_{1,stage}^{2}\,u_{1,in}\dfrac{du_{1,in}}{dw}\right)}{u_{1,in}^{4}} \qquad (13)$$

3.4 Optimization Algorithm

The use of geometrically nonlinear FEA and large number of chosen elements and nodes make the problem computationally very expensive. Since sequential quadratic programming algorithm requires multiple function evaluations in each iteration, and since the method of moving asymptotes (MMA) [11] resolves this issue to some extent by using the dual method, the latter is implemented to carry out the optimization.

4   Results and Discussions

The value of λ is varied uniformly from 0 to 1 in a step of 0.0556 to obtain a series of minimal values for the objective functions are plotted in Fig. (3). Corresponding data is given in Table 1.
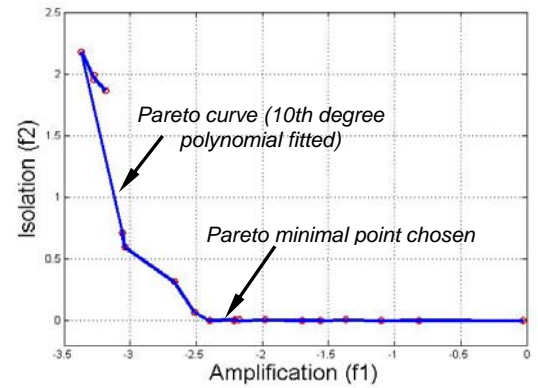

Figure 3: Pareto front generation. The value of λ is varied equally from 0 to 1 and corresponding minimal values of both objective function are plotted on X and Y axis respectively.

The obtained mechanism is analyzed using COMSOL multi-physics software, and the results are shown in Figs. (5-7). Three load cases are identified, namely load along the X axis only, load along the Y axis only, and load along both the X and Y axes simultaneously. In all the three cases, two parameters, namely stage amplification (*SA*) and stage isolation (*SI*) are identified and the results are tabulated in Table 2.

$$SA = \frac{Desired\ Displacement}{Input\ displacement} \qquad (14)$$

$$SI = \frac{Undesired\ Displacement}{Desired\ Displacement} \qquad (15)$$

Ideally, one would like to achieve amplification as high as possible and isolation as low as possible. Here it is found that the amplification achieved is more than 1 when individual loads are applied and it is less than 1 when the loads are acted together. It may be attributed to the additional stiffness that is offered by the compliant mechanism when the loads are acting together.

The optimized topology corresponding to the chosen Pareto minimal point is shown in Fig. (4), and in Table 1 in italics and red colour.

Table 1: Data for Pareto front generation. The red colored one shows the chosen Pareto minimal point.

| S .No	λ	f_1	f_2
1	0	-0.0294	0.0001
2	0.0556	-0.8146	0.0027
3	0.1111	-1.1024	0.0001
4	0.1667	-1.3686	0.0078
5	0.2222	-1.5607	0.0015
6	0.2778	-1.6979	0.0018
7	0.3333	-1.9808	0.0048
8	0.3889	-2.1766	0.0051
9	0.4444	-2.2144	0.0039
10	*0.5000*	*-2.2095*	*0.0090*
11	0.5556	-2.3986	0.0040
12	0.6111	-2.5136	0.0684
13	0.6667	-2.6640	0.3141
14	0.7222	-3.0405	0.5952
15	0.7778	-3.0555	0.7128
16	0.8333	-3.3682	2.1748
17	0.8889	-3.2768	1.9555
18	0.9444	-3.1869	1.8653
19	1.0000	-3.2775	1.9883
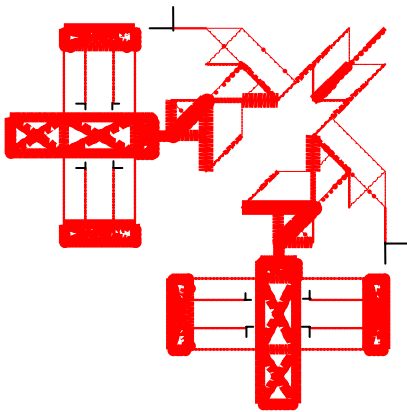
Figure 4: Optimized topology for $\lambda = 0.5$ (Pareto minimal chosen). Fixed points and the point of application of loads are same as given in Fig. (1) and Fig. (2).

Table 2: A summary of the amplification and isolation achieved. The data corresponds to the behavior of the stage in the first quadrant.

Load Case	F_x	F_y	u_{stage}	v_{stage}	u_{input}	v_{input}	SA	SI
1	16	00	2.56	3.41	0.28	-	1.3	0.11
2	00	16	3.41	0.28	-	0.28	1.3	0.11
3	16	16	2.58	2.58	3.07	3.07	0.84	-

4.1 Discussion

4.1.1 Actuation

For making use of the stage as a micro-manipulator a control system is often required. Since the motion of a CM is accurately predictable, one can even incorporate an open-loop control system provided that the actuators are highly reliable and precise. However, most of the high-resolution actuators such as piezoelectric, electro magnetic and hydraulic actuators are either of low range or are very heavy. A large range of motion can be achieved by using a SMA wire actuator. However, highly nonlinear relationship between the current passing through SMA and its displacement makes it inefficient and inaccurate to achieve high precision without a closed-loop control system. Precise control of temperature to effect controlled input is also not easy with SMA actuators. But, we use SMA actuation in this work as a first trial for demonstration.
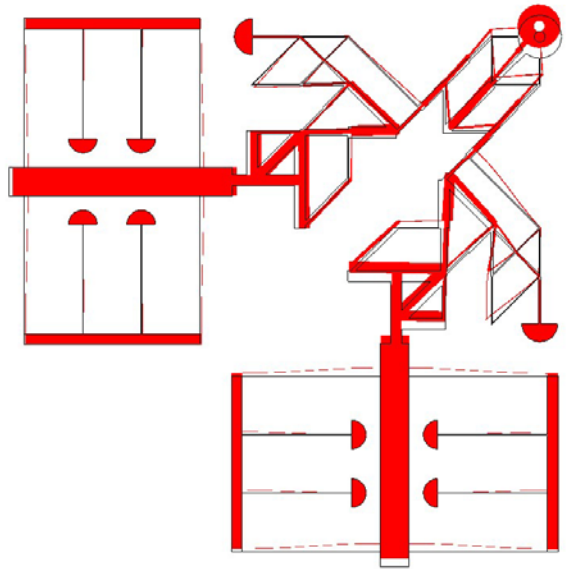

Figure 5: Results of finite element analysis done using COMSOL. Load is applied only along Y axis. Input points and fixed points are same as that of given in Fig. (1) and Fig. (2). $v_{stage} = 3.41mm$ $v_{input} = 2.56mm$ $u_{stage} = 0.28mm$

4.1.2 Computation of forces and displacements.

For positioning the stage at a certain location in the workspace, the displacement of the center of the stage from the neutral position is required. Once the absolute displacements from the initial configuration are obtained, the forces required at both the inputs can be interpolated using the simulation results, shown in Fig. (8) and Fig. (9).

4.1.3 Comparative study

In order to understand the effectiveness of the mechanism obtained, its certain parameters are compared with one of the X-Y stages (Fig. (10)) available in the literature [1]. A normalized parameter, called specific range (SR) [1] is used to compare the effectiveness of various precision instruments. It is defined as the ratio of the range of motion along one axis (either X or Y) to the characteristic length of the stage. Here, since the area covered is not perfectly a square, we modify it as shown in Eq. (16).
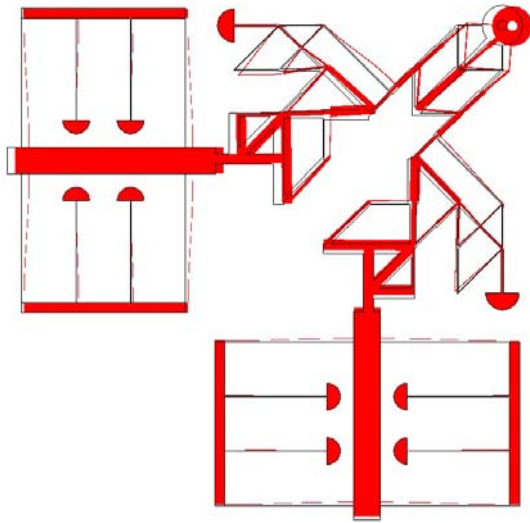
Figure 6: Results of finite element analysis done using COMSOL. Load is applied only along X axis. Input points and fixed points are same as that of given in Fig. (1) and Fig. (2). $u_{stage} = 3.41mm$ $u_{input} = 2.56mm$ $v_{stage} = 0.28mm$
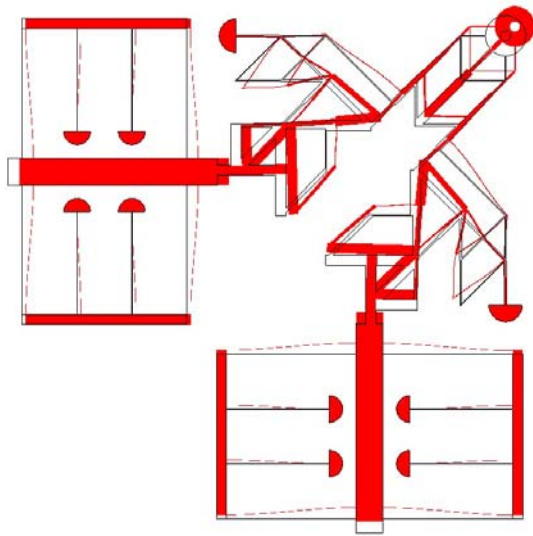

Figure 7: Results of FEA done using COMSOL. Load is applied along both X and Y axis. Input points and fixed points are same as that of given in Fig. (1) and Fig. (2)
$u_{input} = v_{input} = 3.07mm$ $u_{stage} = v_{stage} = 2.58mm$

$$SR = \frac{\sqrt{\text{Area covered}}}{\text{Charecteristic length}} \qquad (16)$$

Other important parameters, namely amplification and stage isolation are compared in Figs. (12-13). Displacement undergone by the chosen stage for various forces at inputs is also simulated in Fig. (11). The area covered by the stage imitates a square albeit not perfectly. This is much worse with the compliant stage obtained (Fig. (9)) in II, III, & IV quadrants. A large amplification and a highly non-linear behavior are obtained in the third quadrant. This is because we have not taken care of this in the

objective function. But this amplification helps to improve the specific range of the obtained X-Y stage in the I quadrant.
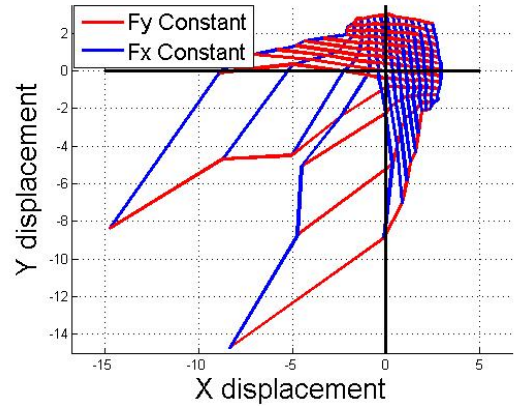

Figure 8: The displacement undergone by the stage for various loads applied at inputs. The loads are applied in steps. Area covered $= 97$ mm^2. Characteristic length of the mechanism$= 150$ mm. Left curve and the bottom most curves represents loads of $F_y = -10:2:16\ N$ and $F_x = -10:2:16\ N$ respectively.
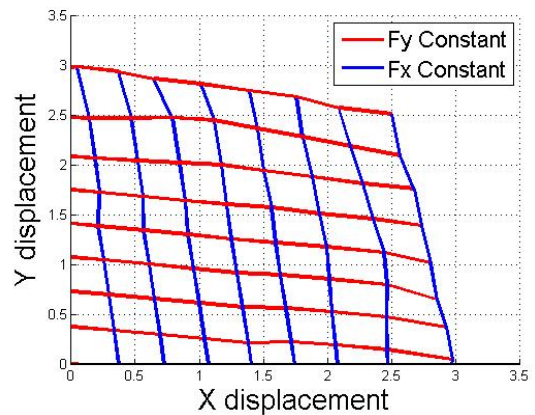

Figure 9: First quadrant of Fig. (8) is shown. Both F_x and F_y are varied from 0 to 16 N in steps of 2 N.

5 Micro-stage Prototype

Spring steel (ENJ42/AISI1080) was chosen as the material for prototyping because of its elastic nature under large-displacement situations. It is also inexpensive. A plastic material such as polypropylene would have been fine but realizing as small a feature as 125 μm, minimum feature size of the mechanism, is not easy unless sophisticated micromachining techniques are used. We used wire-cut Electro Discharge Machining (EDM) to machine the prototype out of spring steel foil. The prototype is shown in Fig. (14).
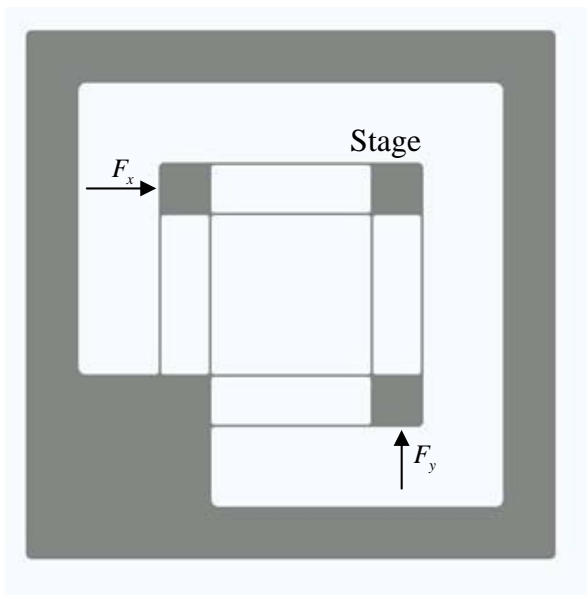
Figure 10: X-Y stage taken for comparison, adapted from Ref [1]. Characteristic length of the mechanism is 150 mm.
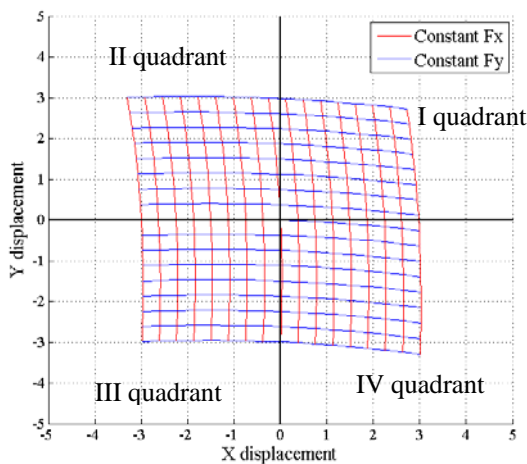

Figure 11: The displacement undergone by the chosen X-Y stage for various loads applied at inputs. The loads are applied in steps. Vertical curves and the horizontal curves represents $F_y = -16:2:16\,N$ and $F_x = -16:2:16\,N$ respectively
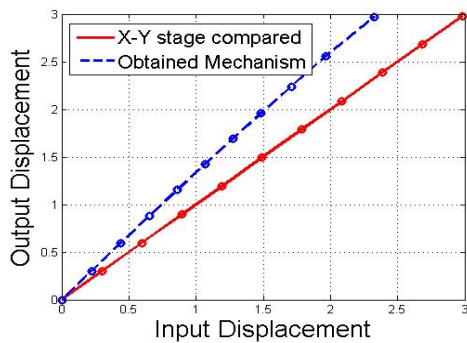

Figure 12: Input displacement vs. output displacement for single axis loading. This gives a measure of amplification achieved.
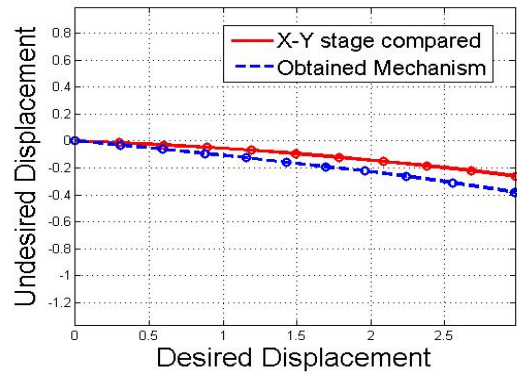

Figure 13: Undesired displacement vs. desired displacement for single axis loading. This gives a measure of stage isolation.

Table 3: Comparison of X-Y stage from literature and the X-Y stage obtained.

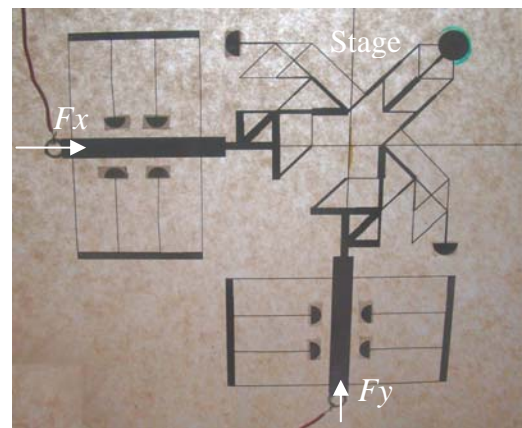| Parameter for comparison	Mechanisms	
	Mechanism Compared	Obtained Mechanism
Specific Range	2.00 %	6.57 %
Stage Isolation	0.10	0.11
Linearity	Nonlinear	Nonlinear
Amplification (for single axis movement)	1.00	1.30

Figure 14: Prototype made of spring steel using a wire cut Electro Discharge Machining (EDM). Loads are applied as shown in the figure. 2 SMA wires are connected along both X and Y axis to actuate the mechanism. The minimum feature size 125 μm and the overall size of the mechanism is 150 mm $\times$ 150 mm

6   Closure

In this paper, a design for large-range compliant X-Y micro stage is obtained by topology optimization. The main feature of the micro stage is that it is obtained my maximizing the workspace and de-coupling the motion in the two directions. The obtained mechanism has a larger spe-

cific range of motion than the existing compliant stages. This is important because actuators that can give large force usually have low stroke. The de-coupling is not perfect but is agreeable to a large extent in the I quadrant. Further modification of the objective function will be pursued to achieve improved de-coupling. The wire-cut EDM was used to make a working prototype using spring steel foils. SMA actuation was used to demonstrate that the stage works as intended. In the future work, manufacturing constraints, stress constraints, and dynamic behavior of the mechanisms will be included in the optimization problem.

Acknowledgment

References

[1] S. Awtar, "Synthesis and Analysis of Parallel Kinematic XY Flexure Mechanisms," *Ph.D. Thesis*, Massachusetts Institute of Technology, 2003.

[2] W. Dong, L.N. Sun, Z.J. Du, "Design of a precision compliant parallel positioner driven by dual piezoelectric actuators," *Sensors and Actuators A*, Vol. 135, 2007, pp. 250–256.

[3] H.H. Pham and I.-M. Chen, "Kinematics, Workspace and Static Analyses of 2-DOF Flexure Parallel Mechanism," *Seventh International Conference on Control, Automation, Robotics and Vision (lCARCV'O2)*, Dec 2002, Singapore.

[4] S.-C. Chen, M.L.Culpepper, "Design of a six-axis micro-scale nanopositioner - μ HexFlex," *Precision Engineering*, Vol. 30, 2006, pp.314–324.

[5] Y.-T. Liu, T. Higuchi, R.-F. Fung, "A novel precision positioning table utilizing impact force of spring-mounted piezoelectric actuator—part II: theoretical analysis," *Precision Engineering*, Vol. 27, 2003, pp.22–31

[6] S.T. Smith and D.G. Chetwynd, 1997, Fundamentals of Ultra precision Mechanism Design Vol. 2, Gordon and Breach Science Publishers.

[7] R.T. Marler and J.S. Arora, "Survey of Multi-objective Optimization Methods for Engineering," *Structures and Multidisciplinary Optimization,* Vol. 26, 2004, pp.369–395.

[8] A. Saxena, G. K. Ananthasuresh, "Topology Synthesis of Compliant Mechanisms for Nonlinear Force-Deflection and Curved Path Specifications," *Journal of Mechanical Design*, Vol. 123, No. 3, March 2001, pp.33-42.

[9] N.D. Mankame, "Investigations on Contact-Aided Compliant Mechanisms," *Ph.D. Thesis*, University of Pennsylvania, 2004.

[10] M.A.Crisfield, 2003, Non-linear Finite Element Analysis of Solids and Structures Vol.1, John Wiley & Sons.

[11] K. Svanberg, "The Method of Moving Asymptotes-A New Method for Structural Optimization," *International Journal for Numerical Methods in Engineering,* Vol. 24, 1987, pp.359-373.